New Phytologist

Research

Hydraulic traits are more diverse in flowers than in leaves

Adam B. Roddy[1], Guo-Feng Jiang[2,3], Kunfang Cao[2,3], Kevin A. Simonin[4] and Craig R. Brodersen[1]

[1]School of Forestry & Environmental Studies, Yale University, New Haven, CT 06511, USA; [2]State Key Laboratory of Conservation and Utilization of Subtropical Agrobioresources, Guangxi University, Nanning, Guangxi 530004, China; [3]Guangxi Key Laboratory of Forest Ecology and Conservation, College of Forestry, Guangxi University, Nanning, Guangxi 530004, China; [4]Department of Biology, San Francisco State University, San Francisco, CA 94132, USA

Author for correspondence:
Adam B. Roddy
Tel: +1 510 224 4432
Email: adam.roddy@yale.edu

Received: *3 December 2018*
Accepted: *11 February 2019*

New Phytologist (2019) **223:** 193–203
doi: 10.1111/nph.15749

Key words: diversity, drought tolerance, evolution, flower, hydraulics, water relations.

Summary

- Maintaining water balance has been a critical constraint shaping the evolution of leaf form and function. However, flowers, which are heterotrophic and relatively short-lived, may not be constrained by the same physiological and developmental factors.
- We measured physiological parameters derived from pressure–volume curves for leaves and flowers of 22 species to characterize the diversity of hydraulic traits in flowers and to determine whether flowers are governed by the same constraints as leaves.
- Compared with leaves, flowers had high saturated water content, which was a strong predictor of hydraulic capacitance in both leaves and flowers. Principal component analysis revealed that flowers occupied a different region of multivariate trait space than leaves and that hydraulic traits are more diverse in flowers than in leaves.
- Without needing to maintain high rates of transpiration, flowers rely on other hydraulic traits, such as high hydraulic capacitance, to maintain turgor pressure. As a result, instead of employing a metabolically expensive but durable carbon (C)-based skeleton, flowers may rely predominantly on a metabolically cheaper, hydrostatic skeleton to keep their structures on display for pollinators, which has important implications for both the costs of reproduction and the biomechanical performance of flowers, particularly during drought.

Introduction

Reproduction is a critical phase in plant life history, in which a strategy of survival and growth transitions to one of maximizing fitness. For most angiosperms, producing flowers is critical to this process because they promote outcrossing through the dispersal and dissemination of pollen, commonly through intimate associations with animal pollinators (Sprengel, 1793, 1996; Crane *et al.*, 1995; Vogel, 1996; Fenster *et al.*, 2004). In order to attract pollinators, flowers are typically borne on aerial shoots at the top of the plant canopy, where temperatures are highest and humidity lowest. Despite their similar canopy placement to leaves, flowers are more ephemeral – typically lasting for only a few days – and predominantly heterotrophic. These two fundamental differences between leaves and flowers have shaped their evolution and provide an excellent case study of how selection on metabolism might influence anatomical and physiological traits.

Flowers are prone to selection by multiple agents, which together have increased the diversity of floral form. Flowers are under selection by their pollinators, and specialized pollination syndromes have promoted diversification and increased morphological disparity (Stebbins, 1951; Fenster *et al.*, 2004; Whittall & Hodges, 2007; Crepet & Niklas, 2009; Chartier *et al.*, 2014, 2017; O'Meara *et al.*, 2016). Flowers also suffer antagonistic relationships with herbivores (Strauss, 1997). Although the incredible diversity of floral morphologies and the rapid rates of floral trait evolution imply that any form is possible (Moyroud & Glover, 2017), flowers are nonetheless constrained by their developmental programs, and pollinator-driven floral evolution is resisted by the physiological costs of producing and maintaining flowers (Berg, 1960; Strauss & Whittall, 2006; Roddy *et al.*, 2013). The existence of diverse, opposing agents of selection could help to promote variation in floral traits within species (Strauss & Whittall, 2006), as well as providing more numerous axes along which species can differentiate, leading to more, equally fit phenotypic solutions (Niklas, 1994).

One commonly acknowledged but rarely quantified agent of selection includes the physiological costs of producing and maintaining flowers. All flowers must supply resources during their development in order to produce and maintain a structure on display for pollinators and that can protect developing embryos. Furthermore, flowers are produced and function in the context of the entire plant, and investment in flowers can often come at the cost of the function of vegetative organs (Bazzaz *et al.*, 1987; Reekie & Bazzaz, 1987a,b,c; Galen, 1999; Galen *et al.*, 1999; Lambrecht & Dawson, 2007; Lambrecht, 2013). The allocation of resources to vegetative growth or reproduction are critical components of plant life-history strategy (Bazzaz *et al.*, 1987). Yet the costs of reproduction are typically quantified solely in terms of biomass (Reekie & Bazzaz, 1987a,b), even though the water costs of producing and maintaining flowers can be high and can feed back to affect both short-term and long-term

physiological functions of leaves (Galen, 1999; Galen *et al.*, 1999; Lambrecht & Dawson, 2007; Roddy & Dawson, 2012). How these nonpollinator agents of selection, such as physiological traits linked to water supply and turgor maintenance, vary among species and might have contributed to floral evolution and diversification has remained largely unstudied. Yet, recent studies have shown strong phylogenetic signal in floral hydraulic traits (Roddy *et al.*, 2016), suggesting that floral diversification may be linked to innovations in floral physiology, just as innovations in leaf anatomy and physiology among the angiosperms are associated with changes in lineage diversity and ecological dominance (Brodribb & Feild, 2010; de Boer *et al.*, 2012; Simonin & Roddy, 2018).

Despite the importance of flowers to both angiosperm ecology and evolution, even basic information about their physiological function is lacking (Gleason, 2018). Because flowers are predominantly heterotrophic and do not assimilate substantial amounts of carbon (C) (but see Galen *et al.*, 1993), it is thought that they may not need to transpire large amounts of water (Blanke & Lovatt, 1993; Liu *et al.*, 2017; Roddy *et al.*, 2018). Flowers tend to have fewer veins and stomata than their conspecific leaves, as a result of a decoupling of the developmental programs controlling these hydraulic traits in leaves and flowers (Lipayeva, 1989; Roddy *et al.*, 2013, 2016; Zhang *et al.*, 2018). However, although flowers may not need high transpiration rates, water can be used to build metabolically cheap, hydrostatic structures that can remain upright when turgid, even if they fail when water is limiting (Vogel, 2013). When resources are limiting, selection would favor certain combinations of traits over others in order to accommodate the multiple selective agents acting on flowers. Because the exchange rate of water for C is high (*c.* 400 : 1; Nobel, 2005), selection may favor flowers that require little C and rely instead on a turgor-driven, hydrostatic skeleton. Thus, the drought strategies of flowers may be directly linked to their biomechanical properties.

The differences between leaves and flowers in metabolism and longevity suggest that flowers may have been released from obeying the same scaling relationships between hydraulic traits as leaves. Whereas leaves must efficiently transport large fluxes of water to maintain transpiration and photosynthesis, flowers, which are heterotrophic, need not transport as much water, and flowers typically have lower densities of veins and stomata (Lipayeva, 1989; Roddy *et al.*, 2013, 2016; Zhang *et al.*, 2018). As a result, flowers may rely on high hydraulic capacitance (i.e. large change in water content per change in water potential) to minimize water potential declines that could otherwise lead to embolism formation and spread (Chapotin *et al.*, 2003; Zhang & Brodribb, 2017; Roddy *et al.*, 2018), a strategy important to vegetative structures as well (Meinzer *et al.*, 2003, 2009; McCulloh *et al.*, 2014). Furthermore, high hydraulic capacitance might delay turgor loss and allow flowers to remain turgid and upright even while water content declines. But the tradeoff to high hydraulic capacitance is that it can delay physiological responses to fluctuating environmental conditions (Nobel & Jordan, 1983). The morphological complexity of flowers and the fact that they need not maintain high transpiration rates (Roddy & Dawson, 2012; Roddy *et al.*, 2016) suggest that flowers and leaves may exhibit a greater diversity of hydraulic and drought strategies than leaves.

One classic method for characterizing hydraulic strategies of leaves has been measurement of the relationship between water content and water potential as leaves slowly desiccate, with the resultant relationship termed a 'pressure–volume curve' (Scholander *et al.*, 1965; Tyree & Hammel, 1972; Schulte & Hinckley, 1985). A variety of parameters related to cell and tissue water relations can be derived from these curves (Table 1), and those most commonly used include the water potential at turgor loss (Ψ_{tlp}), hydraulic capacitance before turgor loss ($C_{1,mass}$), and the bulk modulus of cell wall elasticity (ε_{bulk}). Here we measured pressure–volume relationships in leaves and flowers of 22 species, including magnoliids, monocots, and eudicots, from temperate and subtropical environments to quantify the variation in floral drought responses (Table 2). Based on differences in life span and function, we predicted that flowers would have higher (less negative) turgor loss points (Ψ_{tlp}) and higher hydraulic capacitance than leaves, reflecting a strategy of using hydraulic capacitance to minimize declines in water potential (Chapotin *et al.*, 2003; Roddy *et al.*, 2018). Second, we predicted that, despite differences in longevity and metabolism, flowers would exhibit the same scaling relationships as leaves because both leaves and flowers are governed by the same basic principles of water movement at the cellular level, even if the total fluxes of water being transported mighy differ. Third, we predicted that although traits might exhibit similar scaling relationships in leaves and flowers, because flowers are under different selective regimes they would exhibit greater variation in traits than leaves.

Materials and Methods

Plant material

Species were chosen to include a broad phylogenetic sampling and were selected based on the amenability of measuring water

Table 1 List of traits derived from pressure–volume curve analysis.

Trait	Description	Units
SWC	Saturated water content	g H_2O g^{-1} dry mass
$C_{1,mass}$	Hydraulic capacitance before turgor loss, per dry mass	mol H_2O kg^{-1} MPa^{-1}
$C_{2,mass}$	Hydraulic capacitance after turgor loss, per dry mass	mol H_2O kg^{-1} MPa^{-1}
$N_{s,mass}$	Moles of osmotically active solutes, per dry mass	mol kg^{-1}
ε_{bulk}	Bulk modulus of elasticity	MPa
RWC_{tlp}	Relative water content at the turgor loss point	%
Ψ_{tlp}	Water potential at the turgor loss point	MPa
Ψ_{sft}	Osmotic potential at full turgor	MPa
$W_{T,mass}$	Moles of water extracted between full turgor and turgor loss, per dry mass	mol kg^{-1}

Table 2 List of species and their collection locations.

Species	Family	Habit	Collection location
Magnoliids			
Calycanthus occidentalis Hook. & Arn.	Calycanthaceae	Shrub	UC Botanical Garden, Berkeley, CA, USA
Calycanthus floridus L.	Calycanthaceae	Shrub	Marsh Botanical Garden, New Haven, CT, USA
Calycanthus chinensis (W.C. Cheng & S.Y. Chang) P.T. Li	Calycanthaceae	Shrub	UC Botanical Garden, Berkeley CA, USA
Liriodendron tulipifera L.	Magnoliaceae	Tree	Marsh Botanical Garden, New Haven, CT, USA
Magnolia sieboldii K. Koch	Magnoliaceae	Tree	Arnold Arboretum, Boston, MA, USA
Magnolia stellata (Siebold & Zucc.) Maxim	Magnoliaceae	Tree	Marsh Botanical Garden, New Haven, CT, USA
Magnolia x *loebneri* P. Kache	Magnoliaceae	Tree	Marsh Botanical Garden, New Haven, CT, USA
Monocots			
Anthurium andraeanum Linden ex André	Araceae	Shrub	Guangxi University, Nanning, Guangxi, PRC
Lilium lancifolium Thunb.	Liliaceae		Arnold Arboretum, Boston, MA, USA
Dendrobium sp.	Orchidaceae		Guangxi University, Nanning, Guangxi, PRC
Hemerocallis lilioasphodelus L.	Xanthorrhoeaceae		Marsh Botanical Garden, New Haven, CT, USA
Eudicots			
Clematis sp.	Ranunculaceae	Liana	Marsh Botanical Garden, New Haven, CT, USA
Aquilegia sp.	Ranunculaceae	Shrub	Marsh Botanical Garden, New Haven, CT, USA
Ceiba speciosa (A.St.-Hil.) Ravenna	Malvaceae	Tree	Guangxi University, Nanning, Guangxi, PRC
Rosa sp.	Rosaceae	Shrub	Guangxi University, Nanning, Guangxi, PRC
Bauhinia blakeana Dunn	Fabacaeae	Tree	Guangxi University, Nanning, Guangxi, PRC
Calliandra haematocephala Hassk.	Fabacaeae	Shrub	Guangxi University, Nanning, Guangxi, PRC
Bougainvillea glabra Choisy	Nyctaginaceae	Shrub	Guangxi University, Nanning, Guangxi, PRC
Cornus florida L.	Cornaceae	Tree	Marsh Botanical Garden, New Haven, CT, USA
Bidens pilosa var. *radiata* (Sch.Bip.) Sherff	Asteraceae	Herb	Guangxi University, Nanning, Guangxi, PRC
Stewartia pseudocamellia Maxim.	Theaceae	Tree	Arnold Arboretum, Boston, MA, USA
Rhododendron sp.	Ericaceae	Shrub	Marsh Botanical Garden, New Haven, CT, USA

potentials on their flowers or inflorescences. Because the Scholander-style pressure chamber requires that a minimum length of the petiole or pedicel extend through the compression fitting, we measured only species with pedicels that were at least *c.* 1 cm long. Although we could have included short segments of subtending stems, we avoided this inclusion of material other than that associated developmentally with the flower. Plants were grown outdoors, under well-watered conditions, in botanical gardens and on university campuses (Table 1). These sites and species included both temperate (Marsh Botanical Garden, New Haven, CT, USA; Arnold Arboretum, Jamaica Plain, MA, USA; University of California Botanic Garden, Berkeley, CA, USA) and subtropical (campus of Guangxi University, Nanning, China) sites. Flowering shoots were collected from at least three individuals per species and immediately recut underwater in the early morning and allowed to rehydrate for at least 30 min before individual flowers or leaves were excised for measurement. Potted plants of *Rosa* sp., *Anthurium andraeanum*, and *Dendrobium* sp. were maintained in a well-watered condition before sampling. The morphology of monocot leaves precluded measurements in the pressure chamber, with the exception of *A. andraeanum*. For this species, the entire inflorescence, including both the spathe and the spadix, were measured.

Measurement of pressure–volume parameters

Shoots were allowed to rehydrate and water potentials to equilibrate for at least 2 h before individual flowers or leaves were excised and initial water potentials measured. Initial water potentials were always higher than −0.15 MPa. Following standard methods, pressure–volume curves were constructed for each sample by repeatedly measuring the bulk water potential using a pressure chamber (0.01 MPa resolution; PMS Instruments, Albanay, OR, USA) and subsequently measuring the mass to determine the relationship between water potential and water content (Scholander *et al.*, 1965; Tyree & Hammel, 1972; Schulte & Hinckley, 1985; Sack *et al.*, 2010; Sack & Pasquet-Kok, 2011). Because samples were not fully hydrated (0 MPa) even at the initial measurements, the saturated water content (SWC) was estimated by extrapolating the regression of water mass vs water potential to estimate the water mass at 0 MPa and subsequently dividing by the dry mass. Because rates of water potential change are nonlinear and water potential initially declines rapidly, specimens were only briefly exposed to ambient laboratory air and then enclosed in humidified plastic bags for *c.* 20 min to allow equilibration of water potentials among tissue types. After the specimens reached the point of turgor loss, the duration of their exposure to a dry laboratory atmosphere was lengthened to allow sufficient declines in water potential. The pressure chamber was kept humidified with wet paper towels to prevent evaporation during the water potential measurement. The balancing pressure was determined by slowly increasing the pressure inside the chamber until water was expressed at the cut petiole or pedicel surface, at which time the pressure inside the chamber was slowly decreased to ambient pressure. Immediately afterwards, the specimen was weighed on a balance with a resolution of 0.0001 g. After the conclusion of the measurements, each specimen was oven-dried at 70°C for at least 72 h before determining dry mass. In contrast to prior measurements on leaves, we expressed pressure–volume

parameters on a dry mass basis, rather than on a surface area basis, to facilitate comparisons between flowers and leaves, because the complex morphologies of flowers and their high degree of shrinkage during desiccation prevented accurate measurements of surface area after pressure–volume measurements were complete. Example curves for leaves and flowers are reported in Supporting Information Fig. S1.

Phylogeny

We used PHYLOMATIC (v.3.0) to generate a family-level supertree using the R package 'BRRANCHING'. This supertree is in good agreement with the most recent understanding of the relationships between angiosperm families (Angiosperm Phylogeny Group, 2016). Nodes in the tree were dated using age estimates from Magallón *et al.* (2015), and all branch lengths smoothed using the function 'bladj' in PHYLOCOM (Webb *et al.*, 2008). This dated phylogeny was used in all subsequent phylogenetic analyses. For comparisons of trait values between leaves and flowers (phylogenetic paired *t*-tests), data were not available for monocot leaves, and so the phylogeny was pruned of these species for these analyses.

Data analysis

All statistical analyses were performed in R (v.3.5.0; R Core Team, 2018). Two metrics of phylogenetic signal were calculated for each trait, Pagel's λ and Abouheif's C_{mean} because of the robustness of these two measures (Münkemüller *et al.*, 2012), using the package PHYLOSIGNAL (Keck *et al.*, 2016). Phylogenetic paired *t*-tests (Revell, 2012) were used to compare differences in each trait between leaves and flowers, as well as paired *t*-tests that did not account for shared evolutionary history. Because the leaves of the three monocot species were not measured, these species were entirely omitted from paired *t*-tests, although values for their traits are reported in Fig. 1.

Standard major axis (SMA) regression was used to determine scaling relationships between traits (the function 'sma' in the package SMATR; Warton *et al.*, 2012) because we had no *a priori* information about the direction of causation between variables. To determine whether flowers and leaves exhibited similar scaling relationships, we compared slopes and intercepts between structures. It is possible that flowers and leaves exhibit the same scaling relationships (i.e. equivalent slopes and intercepts) but that, for example, flowers may have higher values of both traits being analyzed. For comparisons of slopes, the likelihood ratio test (LRT) statistic was reported, and for comparisons of elevation and shifts along common slopes, the Wald statistic was reported. For all comparisons except for the relationship between the osmotic potential at full turgor (Ψ_{sft}) and Ψ_{tlp}, data were log-transformed. However, for visualization purposes, data were plotted in arithmetic space with regression lines appropriately transformed. In figure insets, data were plotted in log space for comparison. Because previous studies have pointed to a critical role of hydraulic capacitance in flower water relations, we focused our analysis on elucidating the drivers of this variation, which were thought to include both SWC and ε_{bulk}. Furthermore, the functioning of a hydrostatic skeleton depends on turgor pressure, which is linked to Ψ_{sft}, Ψ_{tlp} and ε_{bulk}. ε_{bulk} is likely influenced by cell wall thickening and, thus, the dry mass. Therefore, SWC may be a critical and easily measurable trait that links tradeoffs between hydraulic capacitance, ε_{bulk} and Ψ_{sft}.

Principal component analysis was used to compare the distributions and volume occupancy in multivariate space of leaves and flowers. Principal components were calculated using the function 'prcomp' on the data for each individual specimen measured to determine the loadings of traits. Means of the principal component (PC) scores for each species and structure were calculated to compare the total multivariate space occupied by flowers and leaves.

Results

Trait-wise differences between leaves and flowers

Although the range of each trait overlapped for flowers and leaves, paired *t*-tests that did and did not correct for shared evolutionary history revealed that flowers and leaves differed significantly in almost every trait (Fig. 2; Table S1). Flowers had significantly higher SWC (nonphylogenetic, $t = 8.28$, df = 25.63, $P < 0.0001$; phylogenetic, $t = 6.18$, $P < 0.0001$), $C_{1,mass}$ (nonphylogenetic, $t = 5.69$, df = 22.85, $P < 0.0001$; phylogenetic, $t = 3.96$, $P < 0.01$), $C_{2,mass}$ (nonphylogenetic, $t = 4.54$, df = 20.99, $P < 0.001$; phylogenetic, $t = 2.86$, $P = 0.01$), moles of osmotically active solutes, per dry mass ($N_{s,mass}$; nonphylogenetic, $t = 3.16$, df = 22.46, $P < 0.01$; phylogenetic, $t = 3.46$, $P < 0.01$), Ψ_{tlp} (nonphylogenetic, $t = 3.66$, df = 34.00, $P < 0.001$; phylogenetic, $t = 4.30$, $P < 0.001$), and Ψ_{sft} (nonphylogenetic, $t = 3.69$, df = 33.71, $P < 0.001$; phylogenetic, $t = 4.76$, $P < 0.001$), but lower ε_{bulk} (nonphylogenetic, $t = 2.01$, df = 27.76, $P = 0.05$; phylogenetic, $t = 2.30$, $P = 0.04$). There were no significant differences between structures in relative water content at the turgor loss point (RWC_{tlp}; nonphylogenetic, $t = 0.33$, df = 33.63, $P = 0.75$; phylogenetic, $t = 0.42$, $P = 0.68$).

Coordination between traits

Capacitance both before ($C_{1,mass}$) and after ($C_{2,mass}$) turgor loss was strongly predicted by SWC (Fig. 3a,b). The relationship between SWC and $C_{1,mass}$ was described by a common slope and intercept among leaves and flowers ($\log(C_{1,mass}) = 1.62 \log(SWC) + 0.25$; $R^2 = 0.81$, $P < 0.0001$; slope, LRT = 0.16, $P = 0.69$; intercept, Wald statistic = 3.46, $P = 0.06$), although flowers were shifted along this common line (Wald statistic = 66.46, $P < 0.0001$). Similarly, SWC predicted $C_{2,mass}$ across species and structures with a single slope ($\log(C_{2,mass}) = 1.70 \log(SWC) + 0.70$; $R^2 = 0.76$, $P < 0.0001$; slope, LRT = 0.03, $P = 0.87$; intercept, Wald statistic = 3.47, $P = 0.06$), although flowers were shifted along this common axis (Wald statistic = 63.58,

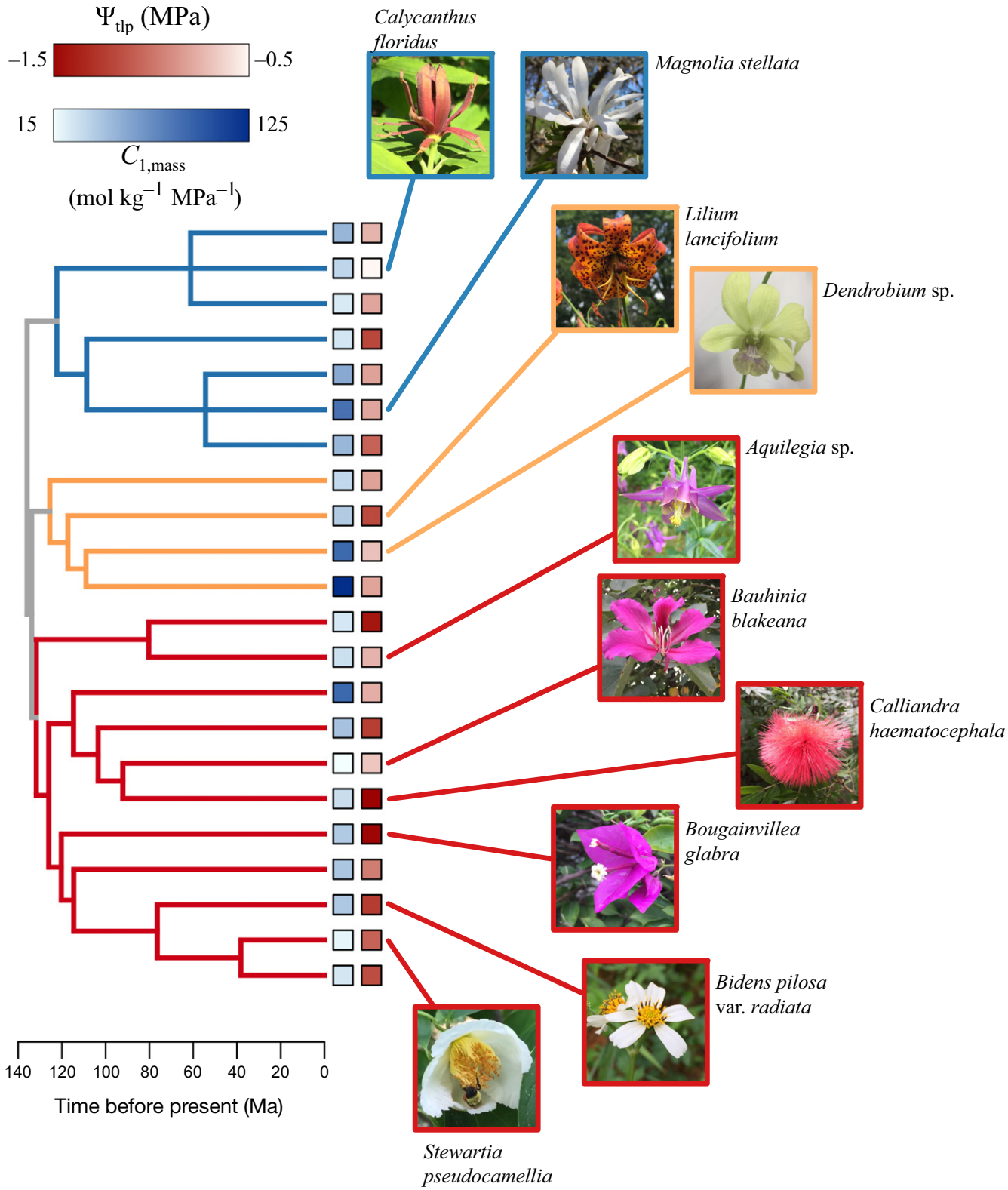

Fig. 1 Phylogenetic relationships of the species sampled with values of hydraulic capacitance before turgor loss ($C_{1,mass}$) and the water potential at turgor loss (Ψ_{tlp}) for flowers mapped on the tips. Photographs of species sampled highlight the morphological diversity. Branches are colored according to clade (blue, magnoliids; orange, monocots; red, eudicots). All photos were taken by ABR.

$P < 0.0001$). A single slope described the relationship between $C_{1,mass}$ and $C_{2,mass}$ across species and structures ($\log(C_{2,mass}) = 1.05 \log(C_{1,mass}) + 0.44$; $R^2 = 0.78$, $P < 0.0001$; Fig. 3c), and flowers were shifted along this common slope towards higher capacitance values (Wald statistic = 53.84, $P < 0.0001$).

There was a highly significant, negative relationship between $C_{1,mass}$ and ε_{bulk} (Fig. 4a), with slope and elevation tests revealing that leaves and flowers have statistically indistinguishable slopes (leaves, $\log(C_{1,mass}) = -1.30 \log(\varepsilon_{bulk}) + 2.45$; $R^2 = 0.77$, $P < 0.0001$; flowers, $\log(C_{1,mass}) = -1.10 \log(\varepsilon_{bulk}) + 2.66$; $R^2 = 0.59$, $P < 0.001$; slope test, LRT = 0.79, $P = 0.37$) but different intercepts (Wald statistic = 69.63, $P < 0.0001$). Furthermore, flowers are shifted along this common scaling axis (Wald statistic = 26.83, $P < 0.0001$).

The relationship between ε_{bulk} and $C_{2,mass}$ showed a similar, significant, negative relationship (Fig. 4b). However, there was no significant difference in slope between leaves and flowers (LRT = 0.009; $P = 0.92$), and a single slope existed among both leaves and flowers ($\log(C_{1,mass}) = -1.90 \log(\varepsilon_{bulk}) + 3.78$; $R^2 = 0.26$, $P < 0.001$).

There was no significant difference between leaves and flowers in the relationship between Ψ_{sft} and Ψ_{tlp} ($\Psi_{sft} = 0.84\Psi_{tlp} + 0.03$; $R^2 = 0.94$, $P < 0.0001$; Fig. 5). Despite the fact that there was no significant difference between leaves and flowers in intercepts (Wald statistic = 0.08, $P = 0.78$), flowers were shifted towards higher values in both traits (Wald statistic = 15.10, $P < 0.001$).

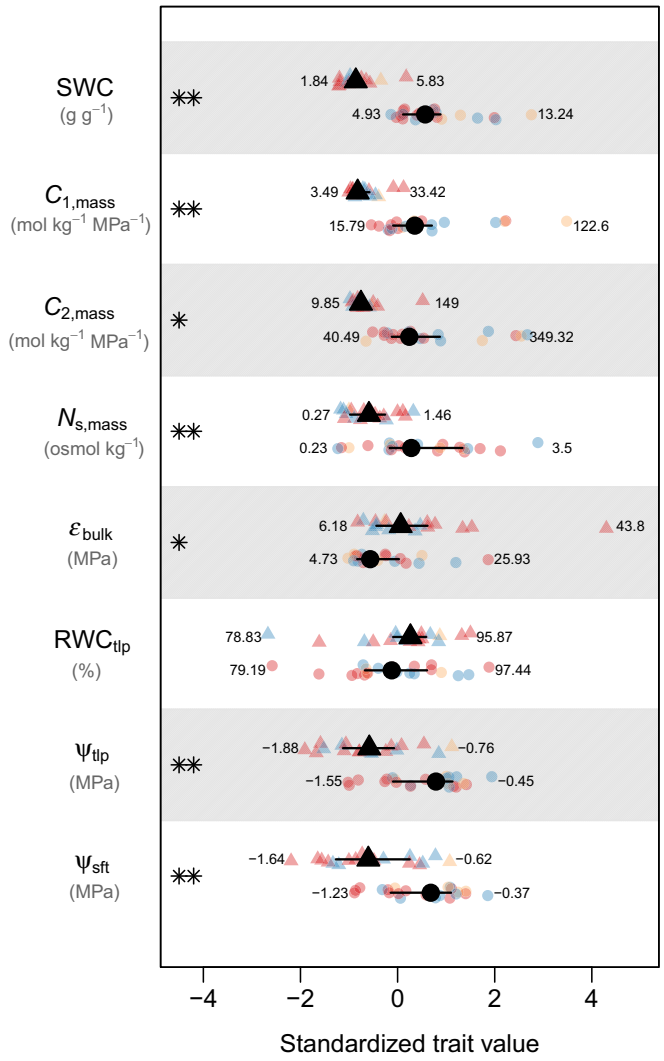

Fig. 2 Standardized differences between leaves (triangles) and flowers (circles) in hydraulic traits. Black points and lines indicate medians ± interquartile ranges for each structure. Colored points are mean values for each species, colored by clade (blue, magnoliids; orange, monocots; red, eudicots). Numbers indicate the maximum and minimum species means of each trait for each structure. Asterisks indicate significant differences between structures in phylogenetically controlled paired *t*-tests: *, $\alpha = 0.05$; **, $\alpha = 0.01$. See the Results section for differences between paired *t*-tests that did and did not correct for shared evolutionary history. SWC, saturated water content; $C_{1,mass}$, hydraulic capacitance before turgor loss, per dry mass; $C_{2,mass}$, hydraulic capacitance after turgor loss, per dry mass; $N_{s,mass}$, moles of osmotically active solutes, per dry mass; ε_{bulk}, bulk modulus of elasticity; RWC$_{tlp}$, relative water content at the turgor loss point; Ψ_{tlp}, water potential at the turgor loss point; Ψ_{sft}, osmotic potential at full turgor.

Multivariate analysis of traits

In multivariate space, the first two principal component axes explained 51% and 27%, respectively, of the variation among leaves and flowers of all species (Fig. 6a,b). Differences in the first axis (PC1) were driven by a tradeoff between ε_{bulk} and traits related to water content and discharge (SWC, $C_{1,mass}$, $C_{2,mass}$). PC2 was driven primarily by a tradeoff between traits related to osmotic concentrations and turgor loss (Ψ_{tlp}, Ψ_{sft}, RWC$_{tlp}$, $N_{s,mass}$). Flowers and leaves differed in the regions of trait space they occupied, consistent with pairwise differences in most traits (Fig. 2). The major differences between leaves and flowers were driven by differences in PC1, with flowers occupying a larger volume of trait space than leaves (Fig. 6b).

Discussion

Here we show that, although similar scaling relationships govern floral and foliar hydraulic traits, flowers encompass a wider diversity of hydraulic trait values than leaves, owing, we hypothesize, to the different selective pressures that have shaped their physiological performance. Whereas selection favored smaller cells in angiosperm leaves that allowed for higher densities of veins and stomata to increase hydraulic conductance and gas exchange rates (Boyce *et al.*, 2009; Brodribb & Feild, 2010; Feild *et al.*, 2011; de Boer *et al.*, 2012; Simonin & Roddy, 2018), flowers have experienced no similar selection for smaller, more densely packed cells capable of higher metabolic rates (Roddy *et al.*, 2013, 2016; Zhang *et al.*, 2018). The relative developmental independence of leaves and flowers, combined with selection for different tissue organization, has enabled the independent evolution of these complex structures (Table 3).

Similar scaling relationships govern leaf and flower hydraulic architecture

Consistent with our first prediction, flowers had significantly higher hydraulic capacitance both before and after turgor loss and higher turgor loss points than leaves (Fig. 2). The relationship between Ψ_{tlp} and Ψ_{sft} was the same for leaves and for flowers, suggesting that methods for rapidly assessing turgor loss

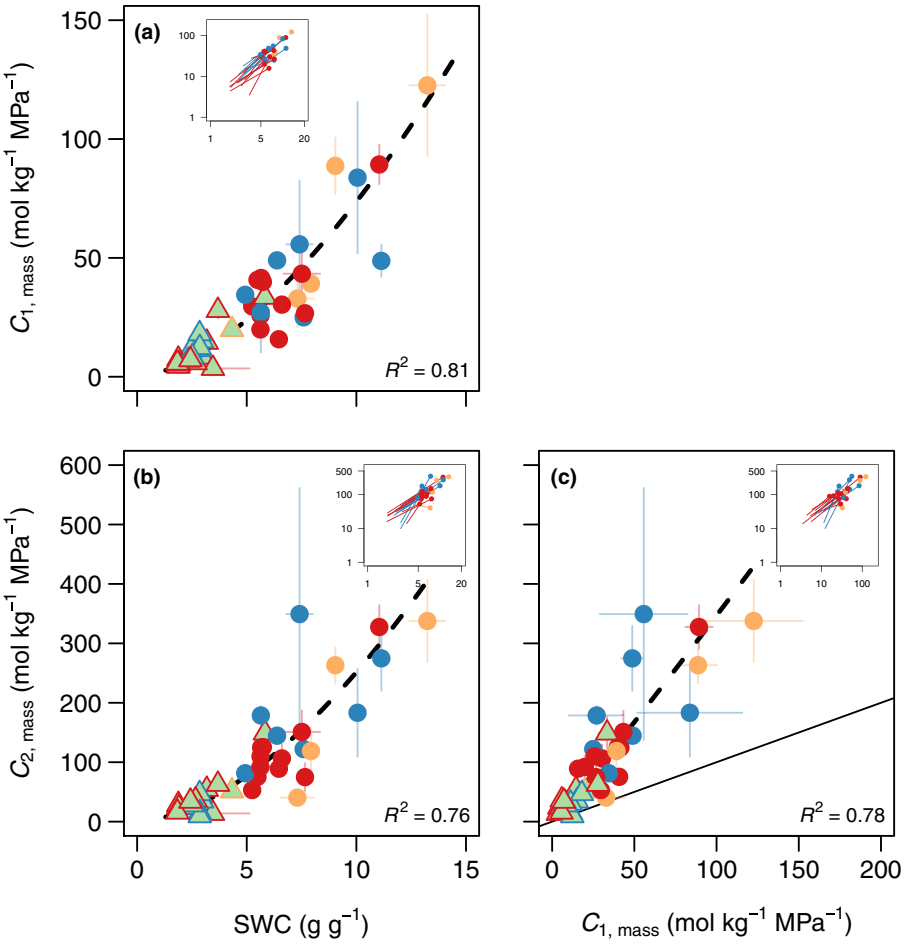

Fig. 3 Relationships between saturated water content (SWC), hydraulic capacitance before turgor loss ($C_{1,mass}$), and hydraulic capacitance after turgor loss ($C_{2,mass}$). Insets show log–log relationships and lines connect conspecific leaves and flowers with endpoints shown for flowers only, for visual clarity. Dashed black lines are standard major axis regressions performed on log-transformed data. (a, b) SWC is a strong predictor of hydraulic capacitance both before and after turgor loss. (c) Hydraulic capacitance after turgor loss is higher than before turgor loss. The solid line is the 1 : 1 line. Error bars represent standard error. Circles, flowers; triangles, leaves (triangle outline color represents leaves' phylogenetic affinity: blue, magnoliids; orange, monocots; red, eudicots).

points in leaves (Bartlett *et al.*, 2012) might be applicable to flowers as well. In addition to hydraulic capacitance, the traits showing the largest differences between flowers and leaves were SWC and $N_{s,mass}$, with flowers having higher trait values for both traits. Indeed, SWC was a strong predictor of hydraulic capacitance before and after turgor loss (Fig. 3), which together with the ε_{bulk} provided the major axis of differentiation between leaves and flowers (Fig. 6). Thus, flowers tend to be composed of cells with flexible cell walls that readily deform during desiccation, facilitating large changes in water content with minimal change in water potential.

We predicted that the same scaling relationships would explain covariation of traits for both leaves and flowers. Our results overall supported this hypothesis, consistent with previous results for traits linked to floral water balance (Figs 3–5; Roddy *et al.*, 2016; Zhang *et al.*, 2018). For example, differences in hydraulic capacitance were driven by consistently higher SWC in flowers compared with conspecific leaves (Fig. 3b,c insets). However, in other cases, although scaling slopes were equivalent for leaves and flowers, the intercepts differed; for a given ε_{bulk}, flowers had higher $C_{1,mass}$. This difference in intercepts between leaves and flowers is a result of differences in SWC (Fig. 3). But where is this extra water per unit dry mass stored in flowers? First, cells in flowers could be larger such that the ratio of vacuole volume to cell wall is higher, and some evidence suggests that epidermal pavement cells and guard cells might be larger in petals than in leaves (Zhang *et al.*, 2018). Additionally, the higher SWC of flowers could be a result of extracellular water stored in the form of mucilage (Chapotin *et al.*, 2003), which we frequently observed in various floral structures (e.g. petals, gynoecia) upon dissection. Furthermore, the presence of extracellular mucilage has been linked to increased hydraulic capacitance in both leaves (Morse, 1990) and flowers (Chapotin *et al.*, 2003), suggesting that storing water as mucilage could be an effective way of avoiding declines in water potential. These results provide strong support that hydraulic structure–function relationships of flowers are the same as or similar to those of leaves, even if leaves and flowers are segregated at different ends of trait spectra.

Axes of floral physiological diversity

In contrast to previous results showing that there is strong phylogenetic signal in hydraulic traits of flowers (Roddy *et al.*, 2016), the traits presented here lack similar phylogenetic structure and exemplify the diversity of extant flowers (Fig. 6; Table 2). In fact, almost every trait was more variable among flowers than among leaves (Fig. 2), which was reflected in the greater variation in multivariate trait space among flowers (Fig. 6). Moreover, despite this greater variation, flowers occupied a nearly distinct region of

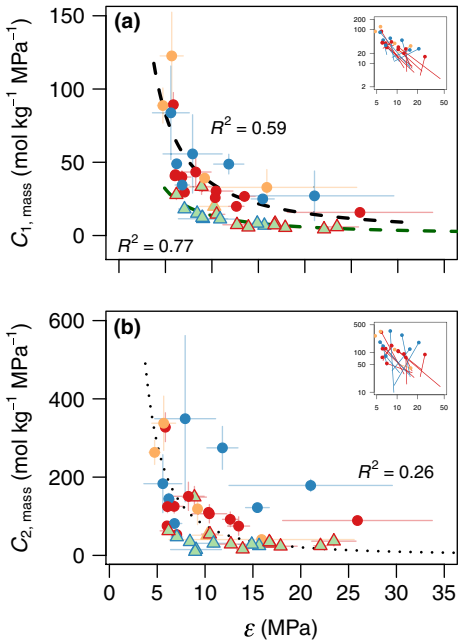

Fig. 4 Relationships between the bulk modulus of elasticity (ε_{bulk}) and hydraulic capacitance before turgor loss ($C_{1,mass}$), and hydraulic capacitance after turgor loss ($C_{2,mass}$). Insets show log–log relationships, and lines connect conspecific leaves and flowers with endpoints shown for only flowers for visual clarity. Dashed lines in (a) indicate standard major axis regressions of log-transformed data for leaves (green dashed line) and flowers (black dashed line) separately. The dotted line in (b) is fitted through data for both leaves and flowers because there was no significant difference between structures. Error bars represent SE. Circles, flowers; triangles, leaves (triangle outline color represents leaves' phylogenetic affinity: blue, magnoliids; orange, monocots; red, eudicots).

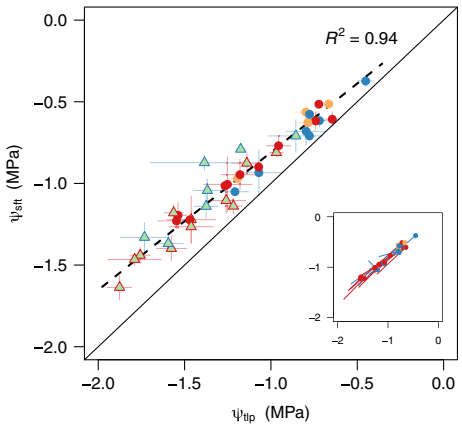

Fig. 5 A single regression explains the relationship between the osmotic potential at full turgor (Ψ_{sft}) and the water potential at turgor loss (Ψ_{tlp}) for leaves and flowers. The dashed black line represents the standard major axis regression for both leaves and flowers, and the solid black line is the 1 : 1 line. Lines in the inset connect conspecific leaves and flowers with endpoints shown for only flowers for visual clarity. Error bars represent SE. Circles, flowers; triangles, leaves (triangle outline color represents leaves' phylogenetic affinity: blue, magnoliids; orange, monocots; red, eudicots).

multivariate trait space, compared with leaves. Among the 22 species studied, leaves of only three species and flowers of only two species existed in the shared region of multivariate trait space. Interestingly, the most similar conspecific structures were those of *A. andraeanum*, the inflorescences of which included a large, leaf-like spathe.

Although the relationships between traits were similar for flowers and leaves, flowers nonetheless diverged in their positions along these axes towards having higher water content and hydraulic capacitance, which has important implications for how flowers maintain water balance. The discharge of water from storage components can decouple water uptake from water loss, effectively preventing steady-state transpiration (Hunt & Nobel, 1987), which is especially important for the measurement of gas exchange and isotope fluxes (Simonin *et al.*, 2013). Buffering declines in water content as a result of transpiration could be important in flowers, which have low vein densities and hydraulic conductance, and which may not be able continuously to supply enough water for transpiration (Roddy *et al.*, 2016, 2018). Furthermore, the high hydraulic capacitance of reproductive organs has the potential to buffer water potential variation in the stem and leaves: diurnal declines in Ψ_{stem} can drive water flow from fruits back into the stem and be replaced nocturnally (Higuchi & Sakuratani, 2006). Hydraulic capacitance ($C_{1,mass}$) can also compensate for the high Ψ_{tlp} common among flowers. By allowing water content to decline with minimal effect on water potential, a high hydraulic capacitance can help to delay water potential declines that lead to turgor loss (Morse, 1990; Meinzer *et al.*, 2009; Roddy *et al.*, 2018). With few stomata and limited control over them, flowers could rapidly lose turgor without the conductive capacity to match their hydraulic supply to their water loss. Detailed studies of the water relations of *Magnolia* (Magnoliaceae) and *Calycanthus* (Calycanthaceae) flowers have shown that, despite having both high hydraulic capacitance and hydraulic conductance that can exceed that of their conspecific leaves, these flowers are nonetheless prone to wilting (Feild *et al.*, 2009a,b; Roddy *et al.*, 2018).

Implications for flower biomechanics

The variation in the hydraulic traits presented here have important implications for the structure and biomechanical performance of flowers. The low dry mass per area of flowers and their high SWC (Fig. 2; Roddy *et al.*, 2016) together suggest that flowers might remain upright as a result of a hydrostatic skeleton maintained by turgor pressure rather than a rigid, C-based skeleton. Structures with relatively high dry mass investment can remain upright even in the absence of turgor pressure, but large, showy flowers like *Bauhinia blakeana* and *Lilium lancifolium*, which have low dry mass investment, must avoid turgor loss in order to remain upright and on display for pollinators. Relying on turgor pressure and a hydrostatic skeleton would increase the susceptibility of floral attraction to water limitation, which could be one explanation as to why intraspecific variation in flower size is strongly influenced by water availability (Lambrecht & Dawson, 2007; Lambrecht, 2013). Although losing water is often considered expensive, the poor conversion rate of water into C (*c.* 400 : 1; Nobel, 2005) could overwhelm the benefit of investing in long-lived C support structures, allowing flowers to

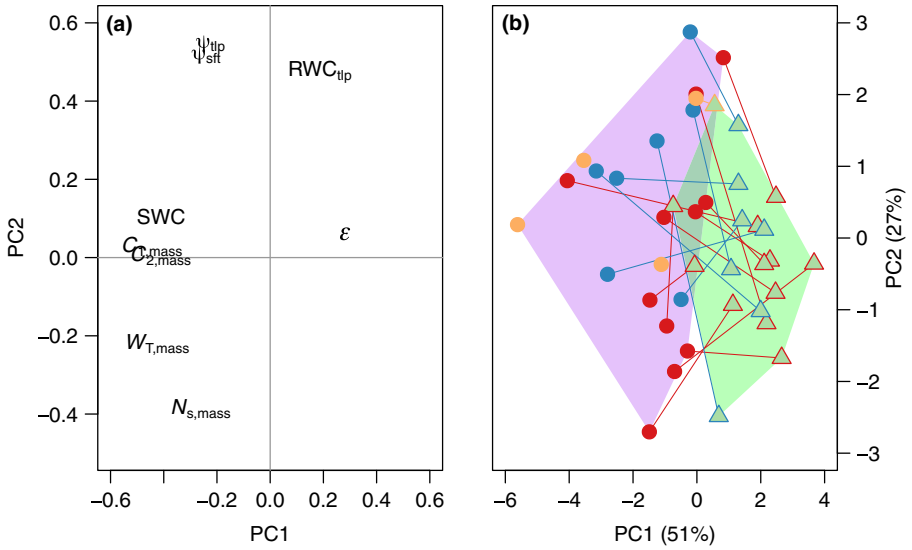

Fig. 6 Results of principal component (PC) analysis performed on raw data for both leaves and flowers. (a) Loadings of the first two PC axes explain a total of 78% of the variation in leaf and flower pressure–volume parameters. SWC, saturated water content; $C_{1,mass}$, hydraulic capacitance before turgor loss, per dry mass; $C_{2,mass}$, hydraulic capacitance after turgor loss, per dry mass; $N_{s,mass}$, moles of osmotically active solutes, per dry mass; ε_{bulk}, bulk modulus of elasticity; RWC_{tlp}, relative water content at the turgor loss point; Ψ_{tlp}, water potential at the turgor loss point; Ψ_{sft}, osmotic potential at full turgor; $W_{T,mass}$, moles of water extracted between full turgor and turgor loss, per dry mass. (b) Mean scores for species and structures in the first two PC axes. Lines connect conspecific leaves (triangles) and flowers (circles), and colors indicate phylogenetic clade (blue, magnoliids; orange, monocots; red, eudicots). The shaded regions indicate the total volume of trait space occupied by leaves (green) and flowers (purple).

be cheaper in terms of C but making them more vulnerable to drought-induced failure. However, relying on turgor pressure to keep corollas upright is not the only method flowers may use to remain on display. Unlike leaves, floral corollas are often not planar, and many petals are curved or fused, which is a common way of increasing flexural stiffness independently of the modulus of elasticity (Vogel, 2013). Although the results presented here are only suggestive of the possible biomechanical strategies and tradeoffs flowers might use, linking the morphological, physiological, and biomechanical aspects of variation in floral form could yield novel insights into the multiple dimensions of floral evolution.

Table 3 Phylogenetic signal in each trait for leaves and flowers, and the trait and phylogenetic independent contrast (PIC) correlations of each trait between leaves and flowers.

	Phylogenetic signal				Correlations	
Trait	Flower C_{mean}	Leaf C_{mean}	Flower λ	Leaf λ	Trait	PIC
SWC	0.17	−0.24	0.63	0.00	−0.25	−0.28
$C_{1,mass}$	0.11	−0.18	0.85	0.00	0.31	0.17
$C_{2,mass}$	0.23*	−0.1	1.12*	0.00	−0.29	−0.27
$N_{s,mass}$	−0.13	−0.14	0.00	0.00	0.04	0.16
ε_{bulk}	−0.10	0.09	0.00	1.34	0.10	0.07
RWC_{tlp}	0.01	−0.08	1.34	0.00	0.28	0.43
Ψ_{tlp}	0.01	−0.16	0.63	0.00	0.22	0.44
Ψ_{sft}	−0.05	−0.10	0.25	0.00	0.26	0.26

SWC, saturated water content; $C_{1,mass}$, hydraulic capacitance before turgor loss, per dry mass; $C_{2,mass}$, hydraulic capacitance after turgor loss, per dry mass; $N_{s,mass}$, moles of osmotically active solutes, per dry mass; ε_{bulk}, bulk modulus of elasticity; RWC_{tlp}, relative water content at the turgor loss point; Ψ_{tlp}, water potential at the turgor loss point; Ψ_{sft}, osmotic potential at full turgor. See Table 2 for the list of species compared. Species × structure trait means and standard error are available in Supporting Information Table S1.
*$P < 0.05$.

Acknowledgements

The authors thank K. Richardson and F. Rosin of the Arnold Arboretum and H. Forbes of the UC Botanical Garden for facilitating access to plant material. K. Niklas provided valuable input on interpretation. JinYan Lei, SuYuan Li, and YiChan Li provided assistance with data collection. M. E. Olson, K. Prats, and two anonymous reviewers provided valuable feedback on previous drafts. ABR was supported by grants from the Yale Institute for Biospheric Studies and the Arnold Arboretum of Harvard University and by a visiting fellowship from the Guangxi Department of Foreign Experts (GX2018019). G-FJ and KC were supported by research grants from the National Science Foundation of China (31470469 and 31860195).

Author contributions

ABR, G-FJ, KAS, KC and CRB designed and performed the research. ABR and G-FJ collected the data. ABR analyzed the data. ABR wrote the manuscript, and all authors edited it.

ORCID

Craig R. Brodersen https://orcid.org/0000-0002-0924-2570
Kunfang Cao https://orcid.org/0000-0002-2253-7189
Guo-Feng Jiang https://orcid.org/0000-0002-3221-8608
Adam B. Roddy https://orcid.org/0000-0002-4423-8729
Kevin A. Simonin https://orcid.org/0000-0002-4990-580X

References

Angiosperm Phylogeny Group. 2016. An update of the angiosperm phylogeny group classification for the orders and families of flowering plants: APG IV. *Botanical Journal of the Linnean Society* **181**: 1–20.

Bartlett MK, Scoffoni C, Ardy R, Zhang Y, Sun S, Cao K, Sack L. 2012. Rapid determination of comparative drought tolerance traits: using an osmometer to predict turgor loss point. *Methods in Ecology and Evolution* **3**: 880–888.

Bazzaz FA, Chiariello NR, Coley P, Pitelka LF. 1987. Allocating resources to reproduction and defense. *BioScience* **37**: 58–67.

Berg RL. 1960. The ecological significance of correlation pleiades. *Evolution* **14**: 171–180.

Blanke MM, Lovatt CJ. 1993. Anatomy and transpiration of the avocado inflorescence. *Annals of Botany* **71**: 543–547.

de Boer HJ, Eppinga MB, Wassen MJ, Dekker SC. 2012. A critical transition in leaf evolution facilitated the cretaceous angiosperm revolution. *Nature Communications* **3**: 1221.

Boyce CK, Brodribb TJ, Feild TS, Zwieniecki MA. 2009. Angiosperm leaf vein evolution was physiologically and environmentally transformative. *Proceedings of the Royal Society of London. Series B, Biological Sciences* **276**: 1771–1776.

Brodribb TJ, Feild TS. 2010. Leaf hydraulic evolution led a surge in leaf photosynthetic capacity during early angiosperm diversification. *Ecology Letters* **13**: 175–183.

Chapotin SM, Holbrook NM, Morse S, Gutiérrez MV. 2003. Water relations of tropical dry forest flowers: pathways for water entry and the role of extracellular polysaccharides. *Plant, Cell & Environment* **26**: 623–630.

Chartier M, Jabbour F, Gerber S, Mitteroecker P, Sauquet H, von Balthazar M, Staedler Y, Crane PR, Schönenberger J. 2014. The floral morphospace – a modern comparative approach to study angiosperm evolution. *New Phytologist* **204**: 841–853.

Chartier M, Löfstrand S, von Balthazar M, Gerber S, Jabbour F, Sauquet H, Schönenberger J. 2017. How (much) do flowers vary? Unbalanced disparity among flower functional modules and a mosaic pattern of morphospace occupation in the order Ericales. *Proceedings of the Royal Society of London. Series B, Biological Sciences* **284**: 20170066.

Crane PR, Friis EM, Pedersen KR. 1995. The origin and early diversification of the angiosperms. *Nature* **374**: 27–33.

Crepet WL, Niklas KJ. 2009. Darwin's second 'abominable mystery': Why are there so many angiosperm species? *American Journal of Botany* **96**: 366–381.

Feild TS, Brodribb TJ, Iglesias A, Chatelet DS, Baresch A, Upchurch GR, Gomez B, Mohr BAR, Coiffard C, Kvacek J *et al.* 2011. Fossil evidence for cretaceous escalation in angiosperm leaf vein evolution. *Proceedings of the National Academy of Sciences, USA* **108**: 8363–8366.

Feild TS, Chatelet DS, Brodribb TJ. 2009a. Ancestral xerophobia: a hypothesis on the whole plant ecophysiology of early angiosperms. *Geobiology* **7**: 237–264.

Feild TS, Chatelet DS, Brodribb TJ. 2009b. Giant flowers of southern magnolia are hydrated by the xylem. *Plant Physiology* **150**: 1587–1597.

Fenster CB, Armbruster WS, Wilson P, Dudash MR, Thomson JD. 2004. Pollination syndromes and floral specialization. *Annual Review of Ecology, Evolution, and Systematics* **35**: 375–403.

Galen C. 1999. Why do flowers vary? *BioScience* **49**: 631–640.

Galen C, Dawson TE, Stanton ML. 1993. Carpels and leaves: meeting the carbon cost of reproduction in an alpine buttercup. *Oecologia* **95**: 187–193.

Galen C, Sherry RA, Carroll AB. 1999. Are flowers physiological sinks or faucets? Costs and correlates of water use by flowers of *Polemonium viscosum*. *Oecologia* **118**: 461–470.

Gleason SM. 2018. A blooming interest in the hydraulic traits of flowers. *Plant, Cell & Environment* **41**: 2247–2249.

Higuchi H, Sakuratani T. 2006. Dynamics in mango (*Mangifera indica* L.) fruit during the young and mature fruit seasons as measured by the stem heat balance method. *Journal of the Japanese Society for Horticultural Science* **75**: 11–19.

Hunt ERJ, Nobel PS. 1987. Non-steady state water flow for three desert perennials with different capacitances. *Australian Journal of Plant Physiology* **14**: 363–375.

Keck F, Rimet F, Bouchez A, Franc A. 2016. phylosignal: an R package to measure, test, and explore the phylogenetic signal. *Ecology and Evolution* **6**: 2774–2780.

Lambrecht SC. 2013. Floral water costs and size variation in the highly selfing *Leptosiphon bicolor* (Polemoniaceae). *International Journal of Plant Sciences* **174**: 74–84.

Lambrecht SC, Dawson TE. 2007. Correlated variation of floral and leaf traits along a moisture availability gradient. *Oecologia* **151**: 574–583.

Lipayeva LI. 1989. On the anatomy of petals in angiosperms. *Botanicheskii Zhurnal* **74**: 9–18.

Liu H, Xu Q-Y, Lundgren MR, Ye Q. 2017. Different water relations between flowering and leaf periods: a case study in flower-before-leaf-emergence *Magnolia* species. *Functional Plant Biology* **44**: 1098–1110.

Magallón S, Gómez-Acevedo S, Sánchez-Reyes LL, Hernández-Hernández T. 2015. A metacalibrated time-tree documents the early rise of flowering plant phylogenetic diversity. *New Phytologist* **207**: 437–453.

McCulloh KA, Johnson DM, Meinzer F, Woodruff D. 2014. The dynamic pipeline: hydraulic capacitance and xylem hydraulic safety in four tall conifer species. *Plant, Cell & Environment* **37**: 1171–1183.

Meinzer F, James SA, Goldstein G, Woodruff D. 2003. Whole-tree water transport scales with sapwood capacitance in tropical forest canopy trees. *Plant, Cell & Environment* **26**: 1147–1155.

Meinzer FC, Johnson DM, Lachenbruch B, McCulloh KA, Woodruff DR. 2009. Xylem hydraulic safety margins in woody plants: coordination of stomatal control of xylem tension with hydraulic capacitance. *Functional Ecology* **23**: 922–930.

Morse S. 1990. Water balance in *Hemizonia luzulifolia*: the role of extracellular polysaccharides. *Plant, Cell & Environment* **13**: 39–48.

Moyroud E, Glover BJ. 2017. The evolution of diverse floral morphologies. *Current Biology* **27**: R941–R951.

Münkemüller T, Lavergne S, Bzeznik B, Dray S, Jombart T, Schiffers K, Thuiller W. 2012. How to measure and test phylogenetic signal. *Methods in Ecology and Evolution* **3**: 743–756.

Niklas KJ. 1994. Morphological evolution through complex domains of fitness. *Proceedings of the National Academy of Sciences, USA* **91**: 6772–6779.

Nobel PS. 2005. *Physicochemical & environmental plant physiology*. New York, NY, USA: Academic Press.

Nobel PS, Jordan PW. 1983. Transpiration stream of desert species: resistances and capacitances for a C_3, a C_4, and a CAM plant. *Journal of Experimental Botany* **34**: 1379–1391.

O'Meara B, Smith S, Armbruster WS, Harder L, Hardy CR, Hileman L, Hufford L, Litt A, Magallón S, Smith S *et al.* 2016. Non-equilibrium dynamics and floral trait interactions shape extant angiosperm diversity. *Proceedings of the Royal Society of London. Series B: Biological Sciences* **283**: 20152304.

R Core Team. 2018. *R: a language and environment for statistical computing*. Vienna, Austria: R Foundation for Statistical Computing.

Reekie EG, Bazzaz FA. 1987a. Reproductive effort in plants. 1. Carbon allocation to reproduction. *American Naturalist* **129**: 876–896.

Reekie EG, Bazzaz FA. 1987b. Reproductive effort in plants. 2. Does carbon reflect the allocation of other resources? *American Naturalist* **129**: 897–906.

Reekie EG, Bazzaz FA. 1987c. Reproductive effort in plants. 3. Effect of reproduction on vegetative activity. *American Naturalist* **129**: 907–919.

Revell LJ. 2012. phytools: an R package for phylogenetic comparative biology (and other things). *Methods in Ecology and Evolution* **3**: 217–223.

Roddy AB, Brodersen CR, Dawson TE. 2016. Hydraulic conductance and the maintenance of water balance in flowers. *Plant, Cell & Environment* **39**: 2123–2132.

Roddy AB, Dawson TE. 2012. Determining the water dynamics of flowering using miniature sap flow sensors. *Acta Horticulturae* **951**: 47–54.

Roddy AB, Guilliams CM, Lilittham T, Farmer J, Wormser V, Pham T, Fine PVA, Feild TS, Dawson TE. 2013. Uncorrelated evolution of leaf and petal venation patterns across the angiosperm phylogeny. *Journal of Experimental Botany* **64**: 4081–4088.

Roddy AB, Simonin KA, McCulloh KA, Brodersen CR, Dawson TE. 2018. Water relations of *Calycanthus* flowers: hydraulic conductance, capacitance, and embolism resistance. *Plant, Cell & Environment* **41**: 2250–2262.

Sack L, Cornwell WK, Santiago LS, Barbour MM, Choat B, Evans JR, Munns R, Nicotra A. 2010. A unique web resource for physiology, ecology and the

environmental sciences: PrometheusWiki. *Functional Plant Biology* **37**: 687–693.

Sack L, Pasquet-Kok J, PrometheusWiki contributors. 2011. *Leaf pressure-volume curve parameters. PrometheusWiki* [WWW document] URL http://prometheuswiki.org/tiki-pagehistory.php?page=Leaf pressure-volume curve parameters&preview=16 [accessed 1 May 2014].

Scholander PF, Bradstreet ED, Hemmingsen E, Hammel H. 1965. Sap pressure in vascular plants: negative hydrostatic pressure can be measured in plants. *Science* **148**: 339–346.

Schulte P, Hinckley T. 1985. A comparison of pressure-volume curve data analysis techniques. *Journal of Experimental Botany* **36**: 1590–1602.

Simonin KA, Roddy AB. 2018. Genome downsizing, physiological novelty, and the global dominance of flowering plants. *PLoS Biology* **16**: e2003706.

Simonin KA, Roddy AB, Link P, Apodaca R, Tu KP, Hu J, Dawson TE, Barbour MM. 2013. Isotopic composition of transpiration and rates of change in leaf water isotopologue storage in response to environmental variables. *Plant, Cell & Environment* **36**: 2190–2206.

Sprengel C. 1793. *Das entdeckte Geheimniss der Natur im Bu und in der Befruchtung der Blumen.* Berlin, Germany: Friedrich Vieweg dem aeltern.

Sprengel C. 1996. Discovery of the secret nature in the structure and fertilization of flowers. In: Lloyd D, Barrett S, eds. *Floral biology*. New York, NY, USA: Springer, 3–43.

Stebbins GL. 1951. Natural selection and the differentiation of angiosperm families. *Evolution* **5**: 299–324.

Strauss S. 1997. Floral characters link herbivores, pollinators, and plant fitness. *Ecology* **78**: 1640–1645.

Strauss S, Whittall J. 2006. Non-pollinator agents of selection on floral traits. In: Harder LD, Barrett SCH, eds. *Ecology and evolution of flowers*. New York, NY, USA: Oxford University Press, 120–138.

Tyree MT, Hammel HT. 1972. The measurements of the turgor pressure and the water relations of plants by the pressure-bomb technique. *Journal of Experimental Botany* **23**: 267–282.

Vogel S. 1996. Christian Konrad Sprengel's theory of the flower: the cradle of floral ecology. In: Lloyd D, Barrett S, eds. *Floral biology*. New York, NY, USA: Springer, 44–62.

Vogel S. 2013. *Comparative biomechanics*. Princeton, NJ, USA: Princeton University Press.

Warton DI, Duursma RA, Falster DS, Taskinen S. 2012. smatr 3–an R package for estimation and inference about allometric lines. *Methods in Ecology and Evolution* **3**: 257–259.

Webb CO, Ackerly DD, Kembel SW. 2008. phylocom: software for the analysis of phylogenetic community structure and trait evolution. *Bioinformatics* **24**: 2098–2100.

Whittall J, Hodges SA. 2007. Pollinator shifts drive increasingly long nectar spurs in columbine flowers. *Nature* **447**: 706–709.

Zhang F-P, Brodribb TJ. 2017. Are flowers vulnerable to xylem cavitation during drought? *Proceedings of the Royal Society of London. Series B, Biological Sciences* **284**: 20162642.

Zhang F-P, Carins Murphy MR, Cardoso AA, Jordan GJ, Brodribb TJ. 2018. Similar geometric rules govern the distribution of veins and stomata in petals, sepals and leaves. *New Phytologist* **219**: 1224–1234.

Supporting Information

Additional Supporting Information may be found online in the Supporting Information section at the end of the article.

Fig. S1 Exemplary relationships between water content and water potential for two species.

Table S1 Species × structure trait values (mean ± SE) calculated from pressure–volume curves.

Please note: Wiley Blackwell are not responsible for the content or functionality of any Supporting Information supplied by the authors. Any queries (other than missing material) should be directed to the *New Phytologist* Central Office.

See also the Commentary on this article by Olson & Pittermann, **223**: 8–10.